

Development 137, 389-394 (2010) doi:10.1242/dev.044164
 © 2010. Published by The Company of Biologists Ltd

Regulation of neural crest cell fate by the retinoic acid and Pparg signalling pathways

Nan Li¹, Robert N. Kelsh², Peter Croucher³ and Henry H. Roehl^{1,*}

SUMMARY

Although the regulation of osteoblast and adipocyte differentiation from mesenchymal stem cells has been studied for some time, very little is known about what regulates their appearance in discrete regions of the embryo. Here we show that, as in other vertebrates, zebrafish osteoblasts and adipocytes originate in part from cephalic neural crest (CNC) precursors. We investigated the roles that the retinoic acid (RA) and Peroxisome proliferator-activated receptor gamma (Pparg) pathways play in vivo and found that both pathways act on CNC to direct adipocyte differentiation at the expense of osteoblast formation. In addition, we identify two distinct roles for RA in the osteoblast lineage: an early role in blocking the recruitment of osteoblasts and a later role in mature osteoblasts to promote bone matrix synthesis. These findings might help to increase our understanding of skeletal and obesity-related diseases and aid in the development of stem cell-based regenerative therapies.

KEY WORDS: Adipocyte, Osteoprogenitor, Osteoblast, Osteoblastogenesis, All trans retinoic acid, Bone, Cephalic neural crest, *osterix* (*sp7*), *tcf7*, Mesenchymal stem cell, Adipoprogenitor, Peroxisome proliferator-activated receptor gamma (Pparg), CCAAT/enhancer binding protein alpha (*Cebpa*), Runt-related transcription factor 2 (*Runx2*; Core binding factor a1), Zebrafish

INTRODUCTION

Age-related osteoporosis is associated with an increase in adipocytes and a reciprocal decrease in osteoblast numbers within bone marrow (Beresford et al., 1992; Burkhardt et al., 1987; Kajkenova et al., 1997; Koo et al., 1998; Meunier et al., 1971; Nuttall and Gimble, 2000; Verma et al., 2002). Both of these cell types differentiate from a bone marrow-derived multipotent precursor called a mesenchymal stem cell (MSC) (Phinney and Prockop, 2007). Differentiation of MSCs into adipocytes and osteoblasts is driven by Peroxisome proliferator-activated receptor gamma (Pparg) and Runt-related transcription factor 2 (*Runx2*; also known as Core binding factor a1), respectively (Komori et al., 1997; Otto et al., 1997; Tontonoz et al., 1994). Intriguingly, mice that lack one copy of *Pparg* have increased bone mass and elevated osteoblast differentiation (Kawaguchi et al., 2005). Furthermore, pharmaceutical activation of *PPARG* as a treatment for diabetes in humans leads to a decrease in bone mass and has been shown to reduce osteoblast differentiation in mice (Akune et al., 2004; Ali et al., 2005; Grey, 2008). Several other pathways have been shown to regulate adipocyte and osteoblast differentiation from MSCs (Zhao et al., 2008). Whereas Leptin, Estrogen, Wnt and TGF β promote osteoblast differentiation while inhibiting adipogenesis, *Pparg* has the opposite effect. In addition, the transcription factor *Tafazzin* is known to act in MSCs to promote osteoblastogenesis by activating *Runx2* and inhibiting *Pparg* (Hong et al., 2005). Although the mutually exclusive relationship of these two lineages suggests the existence of a bipotent adipo/osteoprogenitor, there is no strong evidence to support this hypothesis.

Recent studies in zebrafish have highlighted its potential as a tool for the analysis of obesity (Flynn et al., 2009; Liu et al., 2007; Schlegel and Stainier, 2006; Song and Cone, 2007; Yang et al., 2008). In addition, several mutant zebrafish lines have been shown to accurately model human skeletal diseases (Clement et al., 2008; Fisher et al., 2003; Lang et al., 2006). Here we analyse the role that the retinoic acid (RA) and *Pparg* pathways play in specifying osteoblast and adipocyte cell fate choices in the cephalic neural crest (CNC). Our findings shed light on how neural crest cells diversify in vivo and might increase our understanding of human diseases such as osteoporosis, diabetes and obesity. These results might also aid in the advancement of new technologies based upon neural crest stem cells (Delfino-Machin et al., 2007; Dupin et al., 2007).

MATERIALS AND METHODS

Oil Red, Alcian Blue and Alizarin Red staining

For Oil Red staining, fish were fixed in 4% paraformaldehyde (PFA) in PBS overnight at 4°C, washed once in PBST (PBS containing 0.1% Tween 20) for 5 minutes, stained with filtered 0.3% Oil Red O (Sigma, O0625) in 60% propan-2-ol for 2 hours, rinsed in PBST and mounted in 75% glycerol. Alcian Blue staining was performed as described (Clement et al., 2008). For Alizarin Red staining, fish were fixed as above, stained overnight in 0.96 ml 0.5% KOH with 0.04 ml saturated Alizarin Red (0.1% Alizarin Red S in 100% ethanol), rinsed and mounted as above.

RNA in situ hybridisation

In situ hybridisation was performed as described (Li et al., 2009; Thisse and Thisse, 2008). The *cebpa* (*CCAAT/enhancer binding protein alpha*) probe was prepared from Image clone 6793849 using M13 forward and reverse primers to prepare the template and T7 RNA polymerase for RNA synthesis. The *twist2* probe was prepared from Image clone 7254680 using primers PME18S F (5'-TGTACGGAAGTGTACTTCTGCTC-3') and PME 18S rev T3 (5'-GGATCCATTAACCCTCACTAAAGGGAAGCCGCGACCTGCAGCTC-3') to prepare the template and T3 RNA polymerase for RNA synthesis.

Fluorescent in situ hybridisations were performed as above with the following modifications: anti-DIG POD (Roche, 11207733910) at 1:500 in 2% Blocking Reagent (Roche, 11096176001) in maleic acid buffer was used in conjunction with detection by a 30-minute incubation in Cyanine 3 Tyramide solution (Perkin Elmer, NEL744001KT). After rinsing several

¹MRC Centre for Developmental and Biomedical Genetics, Addison Building, Western Bank, University of Sheffield, Sheffield, S10 2TN, UK. ²Centre for Regenerative Medicine, Department of Biology and Biochemistry, University of Bath, Claverton Down, Bath, BA2 7AY, UK. ³Academic Unit of Bone Biology, Section of Musculoskeletal Science, University of Sheffield Medical School, Beech Hill Road, Sheffield, S10 2RX, UK.

*Author for correspondence (h.roehl@sheffield.ac.uk)

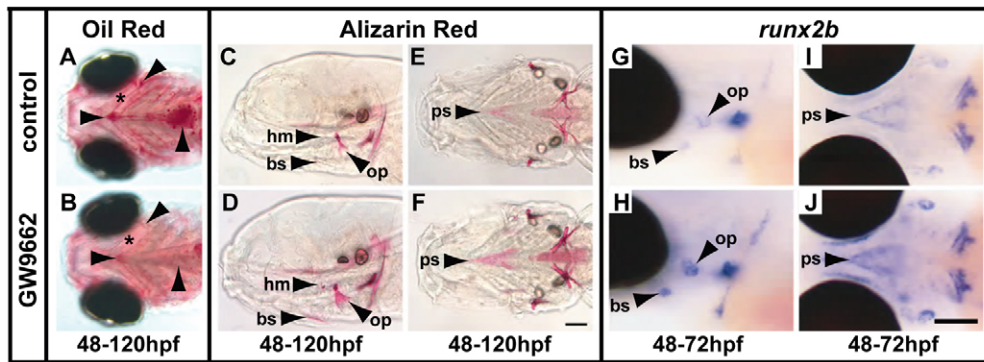


Fig. 1. The Pparg inhibitor GW9662 blocks adipocyte formation while enhancing osteoblast differentiation. (A,B) Ventral views of Oil Red staining showing that lipid droplet accumulation throughout the zebrafish embryo head and cardiac region is strongly diminished by GW9662 treatment for 72 hours. Droplet accumulation (arrowheads) is highest at either end of the ceratohyal cartilage element (asterisk) and around the heart. (C-F) Alizarin Red staining shows that ossification is enhanced after GW9662 treatment for 72 hours. Dermal bones (bs, branchiostegal ray 3; ps, parasphenoid; op, opercle) and a cartilage bone (hm, hyomandibula) show increased levels of ossification. Side views (C,D) and ventral views (E,F) are shown. The eyes have been removed for clarity. Quantification for this experiment is shown in Table S1 in the supplementary material. (G-J) *runx2b* expression is strongly upregulated after 24 hours of GW9662 treatment. The opercle, branchiostegal ray 3 and the parasphenoid primordia all show more intense staining (H,J), consistent with the increase in ossification seen by 120 hpf (D,F). Scale bars: 100 μ m in F for A-F and in J for G-J.

times in PBST, the embryos were re-blocked and stained using standard protocols to detect GFP. Anti-GFP was used at 1:500 (Torrey Pines Biolabs, TP401) and the Alexa 488-conjugated anti-rabbit secondary antibody was used at 1:200 (Molecular Probes). The samples were mounted in Vectashield plus DAPI (Vector Laboratories, H1200) and scanned on an Olympus FV-1000 using a 60 \times oil-immersion lens (1.2 numerical aperture) with sequential scans and optimal pinhole settings.

Chemical treatments

GW9662 (Sigma, M6191) was used at 5 μ M in embryo media (prepared from a frozen 10 mM stock in DMSO). Except where noted (see Fig. 3D and Table S3 in the supplementary material), 4-diethylaminobenzaldehyde (DEAB; Sigma, 31830) was used at 50 μ M (made from a fresh 10 mM stock in DMSO). RA (Sigma, R2625) was used at 0.5 μ M as described (Begemann et al., 2001). Fish were treated in the dark at 28.5°C. Treatments were begun after 48 hpf because this is when *runx2b* and other early osteoblast markers become more restricted to bone condensations.

RESULTS AND DISCUSSION

Pparg is a key regulator of the early adipocyte and osteoblast lineages

Although adipocyte differentiation has been studied in cell culture, nothing is known about the embryonic regulation of adipogenesis (Rosen and MacDougald, 2006). In order to begin to address this problem, we screened small molecules known to affect adipogenesis in mammalian systems, and found that one drug, GW9662, strongly reduces lipid droplet formation in zebrafish. GW9662 is an antagonist of the nuclear hormone receptor Pparg, a regulator of adipocyte differentiation from MSCs (Leesnitzer et al., 2002). Pparg has been shown to promote adipogenesis while inhibiting osteoblast differentiation in mice and humans (Akune et al., 2004; Ali et al., 2005; Grey, 2008). We found that GW9662 treatment for 72 hours inhibits lipid droplet accumulation in cephalic and cardiac regions at 120 hours post-fertilisation (hpf) (Fig. 1A,B). The same treatment resulted in an increase in perichondral (cartilage bone) and dermal (achondral) ossification at 120 hpf (Fig. 1C-F and see Table S1 in the supplementary material). The maxilla, dentary, hyomandibula and ceratohyal, which are usually not present at 120 hpf, were often well ossified in treated animals. In addition, ossification levels of

existing bones (e.g. the opercle and brachioistegal rays) was stronger after GW9662 treatment. Overall, the level of ossification seen at 120 hpf after treatment resembled that of untreated animals at 144 hpf. To determine whether this result was due to a direct effect on osteoblast differentiation, we looked at the expression of *runx2b*, which is an early marker of the osteoblast lineage that also marks a subpopulation of chondrocytes at this stage in development (Flores et al., 2004; Li et al., 2009; van der Meulen et al., 2005). Expression of *runx2b* becomes more restricted to the osteoblast lineage from 48 hpf onwards (Li et al., 2009). GW9662 treatment for 10 or 24 hours resulted in a dramatic increase in *runx2b* expression (Fig. 1G-J and see Fig. S1A-D in the supplementary material), indicating that this initial step in osteoblastogenesis is enhanced. These results suggest that Pparg plays a conserved role in the differentiation of embryonic and adult adipocytes and osteoblasts.

RA signalling is required for adipocyte differentiation in vivo

Another small molecule that regulates adipogenesis is all-trans retinoic acid (RA). RA is crucial, for example, for the differentiation of human embryonic stem cells into adipocytes (Phillips et al., 2003). We tested whether endogenous RA signalling is required for differentiation of adipocytes in vivo. First, we examined the *neckless* (*nls*) mutant, which encodes the RA synthesis enzyme retinaldehyde dehydrogenase type 2 (*Aldh1a2*) (Begemann et al., 2001). We found that *nls*^{-/-} fish do not form oil droplets at day 5 (Fig. 2A,B). We next used *cebpa* as a marker for the adipocyte lineage (Linhart et al., 2001; Umek et al., 1991). *cebpa* is expressed in the liver, gut and pronephric duct at 36 hpf (Thisse et al., 2001). Starting at 48 hpf, *cebpa* begins to be expressed in the pharyngeal arches in regions that will later form oil droplets (Fig. 2). We found that *nls*^{-/-} fish lack *cebpa* expression in the head at 60 hpf (Fig. 2C,D). The *nls*^{-/-} mutation is known to cause widespread patterning defects in the head, shoulder and fin regions of the zebrafish (Begemann et al., 2004; Begemann et al., 2001; Gibert et al., 2006; Kazakova et al., 2006; Linville et al., 2004). To rule out the possibility that the reduction in *cebpa* expression seen in *nls*^{-/-} fish is due to an earlier patterning defect,

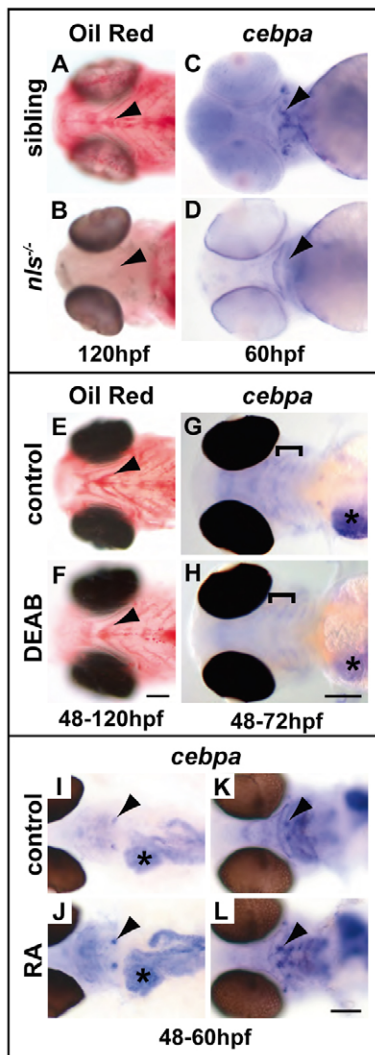


Fig. 2. RA signalling is required for adipocyte differentiation.

(A,B) Ventral views showing that lipid droplet accumulation throughout the head and cardiac region is lost in *nls*^{-/-} fish at 120 hpf. Arrowheads point to droplets present in cells near to the distal end of the ceratohyal cartilage that are present in wild-type (A) and absent in *nls*^{-/-} (B) fish. (C,D) Ventral views showing that expression of the adipocyte differentiation marker *cebpa* is strongly reduced in *nls*^{-/-} fish at 60 hpf. Arrowheads point to a cluster of *cebpa*-positive cells at the distal end of the ceratohyal cartilage (C) that is lost in *nls*^{-/-} embryos (D). Arrowheads point to droplets present in cells near to the distal end of the ceratohyal cartilage that are present in wild-type (C) and absent in *nls*^{-/-} (D) fish. (E,F) Ventral views showing that lipid droplet accumulation throughout the head and cardiac region is reduced after treatment with DEAB. Arrowheads point to droplets present in cells near to the distal end of the ceratohyal cartilage element (E) that are reduced in DEAB-treated fish (F). (G,H) Dorsal views showing that *cebpa* expression throughout the head and liver is reduced after treatment with DEAB. Brackets indicate the area of diffuse expression in the pharyngeal region (G) that is reduced in treated fish (H). The liver also shows a strong reduction in *cebpa* expression levels after DEAB treatment (asterisk). (I-L) Retinoic acid (RA) treatment upregulates expression of *cebpa* after 12 hours. Dorsal flat-mounted fish showing that *cebpa* expression is particularly enhanced in two clusters of cells on either side of the heart (arrowheads in I and J) and liver (asterisk). Ventral views show enhanced expression in the pharyngeal arches, especially at the distal ends of the ceratohyal cartilage (arrowheads in K and L). Scale bars: 100 μ m.

we treated fish with the retinaldehyde dehydrogenase inhibitor DEAB and found that treatment from 48-120 hpf results in a marked decrease in lipid droplet accumulation (Fig. 2E,F) and treatment from 48-72 hpf reduces *cebpa* expression in the pharyngeal arches and liver (Fig. 2G,H). Finally, we tested whether exogenous RA could drive adipogenesis and found that treatment for 12 hours resulted in an upregulation of *cebpa* expression at 60 hpf (Fig. 2I-L). Together, these data indicate that RA induces adipogenesis during zebrafish early development.

RA signalling plays two distinct roles in the osteoblast cell lineage

Given our finding that Pparg regulates early adipogenesis and osteoblastogenesis reciprocally, we wondered whether RA could also play a similar role. The role of RA in osteoblastogenesis has been studied extensively in vitro and it has been shown to both promote and inhibit differentiation, as well as to drive bone matrix synthesis (Ahmed et al., 2000; Benayahu et al., 1994; Choong et al., 1993; Manji et al., 1998; Ohishi et al., 1995; Song et al., 2005; Wiper-Bergeron et al., 2007). Although variation between cell lines, the markers tested and experimental regimes might offer an explanation for these differing results, a clear consensus as to the role of RA has not emerged. Two recent studies in zebrafish have also shown that RA promotes the activity of osteoblasts during bone mineralisation in vivo (Laue et al., 2008; Spoorendonk et al., 2008). To further investigate the role of RA in osteoblast differentiation in vivo, we pulse treated embryos from 48-52 hpf, before the skull bones have begun to ossify. We found that even after 96 hours of recovery (at 144 hpf), many bones were reduced or absent (Fig. 3A,B and see Table S2 in the supplementary material). In particular, the entopterygoid, maxilla and dentary, which are usually well ossified by 144 hpf, were absent in most treated fish. Furthermore, an early pulse treatment with DEAB increased the ossification of both dermal and cartilage bones (Fig. 3C,D and see Table S3 in the supplementary material). These results suggest that RA has an inhibitory effect on early osteoblastogenesis.

To test this model directly, we analysed the impact that RA has on a set of early osteoblast differentiation markers. *tcf7*, *twist2* and *runx2b* are all thought to be key regulators of early osteoblast differentiation (Bialek et al., 2004; Flores et al., 2004; Li et al., 2009; Spoorendonk et al., 2008; van der Meulen et al., 2005). We found that all three of these genes are downregulated when embryos are treated at 48 hpf for 4 hours (Fig. 3E,F,H,I,K,L). *osterix* (*osx*; *sp7* – Zebrafish Information Network), which marks an intermediate stage of differentiation (Li et al., 2009; Nakashima et al., 2002), was also downregulated by RA. Treatments with DEAB caused the opposite response, as expected (Fig. 3G,J,M,P). This rapid response suggests that RA might act directly on the transcription of these genes. To investigate this possibility, we fixed animals after 2 hours of RA treatment and found that whereas early markers were downregulated, *osx* was unaffected (see Fig. S2 in the supplementary material). Since *Osx* transcription requires *Runx2* in mice (Nakashima et al., 2002), it is possible that the reduction in *osx* expression seen after 4 hours of RA treatment is due to depletion of *Runx2*, rather than being a direct effect. Taken together, these results suggest that endogenous RA signalling blocks the recruitment of precursors to the osteoblast lineage by reducing transcription of early regulators of osteoblast differentiation.

Our results contrast with the finding that RA promotes the bone matrix synthesis activity of osteoblasts in vivo (Laue et al., 2008; Spoorendonk et al., 2008). In order to reconcile our results with

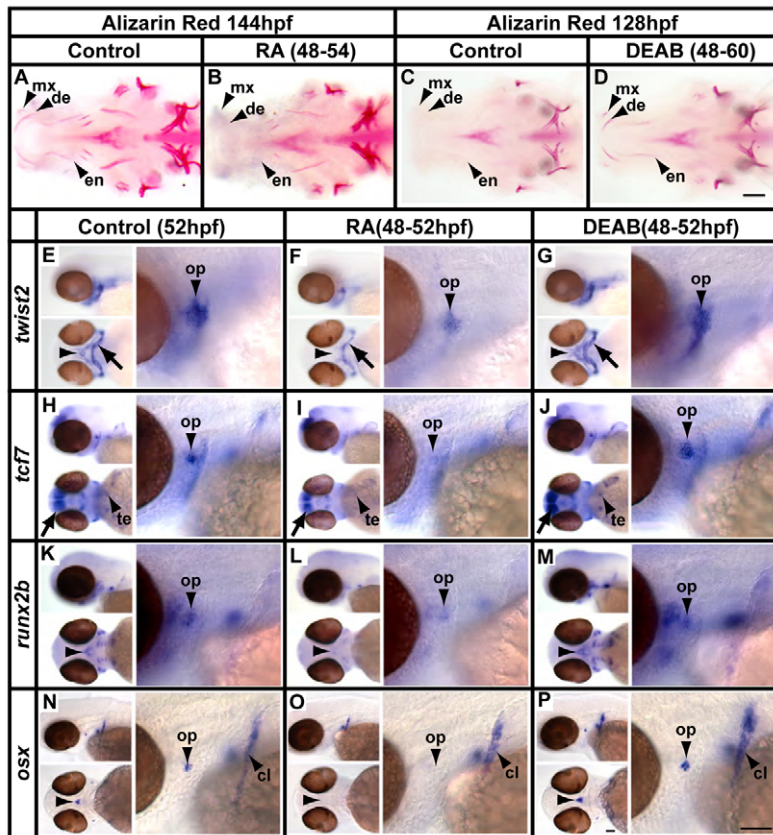


Fig. 3. RA signalling blocks early osteoblast differentiation.

(A-D) Alizarin Red staining at 144 hpf shows that normal levels of ossification (A) are reduced by RA pulse treatment from 48-54 hpf (B). Alizarin Red staining at 128 hpf shows that pulse treatment with DEAB at 10 μ M (D) enhances ossification when compared with control fish (C). Arrowheads point to the maxilla (mx), dentary (de) and entopterygoid (en) (which are all dermal bones). The eyes have been removed for clarity.

Quantification for these experiments is shown in Tables S2 and S3 in the supplementary material. (E-P) Expression of *twist2*, *tcf7*, *runx2b* and *osx* is reduced by RA treatment (F,I,L,O) and enhanced by DEAB treatment (G,J,M,P) as compared with the control (E,H,K,N). Each panel shows side and dorsal views at low magnification (left) and a high-magnification side view of the opercle condensation (right). In the control, *twist2* (E) is expressed strongly in the opercle (op), entopterygoid (not shown) and parasphenoid (arrowhead), as well as broadly in the distal region of the second arch (arrow). *tcf7* (H) is expressed in the opercle and teeth (te), as well as in the brain (arrow). *runx2b* (K) is expressed in the opercle and parasphenoid, as well as in other skeletal elements. *osx* (N) is expressed in the opercle, parasphenoid, cleithrum (cl) and teeth (not shown). Scale bars: 50 μ m.

these findings, we investigated the effects of RA on later stages of development, after much of the skeleton has begun to ossify. In agreement with the previous studies, we found that a pulse treatment with RA when mature osteoblasts are present (at 84-96 hpf) resulted in a strong increase in ossification at 144 hpf (see Fig. S3A,B in the supplementary material). In addition, expression of *collagen 1a1* (*coll1a1*) in osteoblasts at 86 hpf was upregulated after just 2 hours of treatment (see Fig. S3C-E in the supplementary material). As *Coll1a1* is a component of the bone matrix, this suggests that RA activates bone matrix synthesis in osteoblasts. However, when we tested the expression of *runx2b*, we found that expression is strongly downregulated by RA treatment, as shown for earlier time points (see Fig. S3I,J in the supplementary material). Consistent with these results, inhibition of endogenous RA signalling with DEAB gave the opposite response (see Fig. S3K in the supplementary material).

These findings suggest that RA signalling plays at least two roles in the osteoblast lineage: an early role in blocking the recruitment of osteoblasts and a later role in mature osteoblasts to promote bone matrix synthesis. A similar role for RA has been proposed in the regulation of chondrogenesis (Weston et al., 2003). Given that constitutive expression of *Runx2* in mice leads to osteopenia and blocks osteoblast maturation, it is likely that *Runx2* expression must be downregulated for the completion of differentiation (Kanatani et al., 2006). Thus, the early and late roles for RA might in part involve repression of the same set of 'early osteoblast differentiation' genes. It is interesting to speculate that in regions of bone growth and repair, RA availability is initially low to allow recruitment of osteoblasts, then, once osteoblasts are present, RA levels are raised to activate ossification and block the differentiation of more

osteoblasts. Since mature osteoblasts have been shown to express high levels of retinaldehyde dehydrogenase type 2 (Allen et al., 2002), it is possible that in certain circumstances osteoblasts synthesise RA in order to autoregulate their own recruitment and activity.

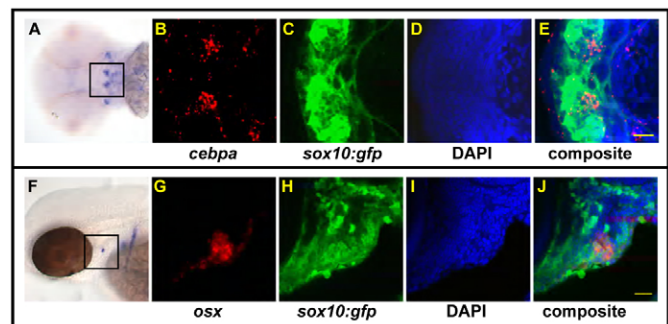


Fig. 4. Cephalic neural crest gives rise to adipocytes and osteoblasts.

(A-E) *cebpa* and *sox10:gfp* are co-expressed in the same cells at 54 hpf. (A) Ventral view of a zebrafish embryo with *cebpa* detection by chromogenic substrate. The boxed area indicates the region shown in B-E. *cebpa* (B) and *sox10:gfp* (C) are co-expressed in the same cells (overlay in E). The nuclear dye DAPI is used as a counterstain to show that not all cells express each marker and that the optical sections are less than one cell diameter (D). (F-J) *osx* and *sox10:gfp* are co-expressed in the same cells at 54 hpf. (F) Side view of a fish with *osx* detection by chromogenic substrate. The boxed area indicates the region shown in G-J. *osx* (G) and *sox10:gfp* (H) are co-expressed in the same cells (overlay in J). (I) Staining with the nuclear dye DAPI. Scale bars: 10 μ m.

Zebrafish cephalic neural crest gives rise to both osteoblasts and adipocytes

Given that tetrapod CNC differentiates into both adipocytes and osteoblasts *in vivo* (Billon et al., 2007; Le Douarin et al., 2004), we decided to test whether the same is true in zebrafish. To identify CNC we utilised a *sox10:gfp* transgenic line [*Tg(-4.9sox10:eGFP)^{ba2}*] as a marker (Carney et al., 2006) and determined whether cells expressing *sox10:gfp* also express *cebpa* or *osx*. We found that at 54 hpf both markers are expressed in CNC cells (Fig. 4A–J), indicating that both adipocytes and osteoblasts originate from a common precursor that is found within the CNC. Since the first embryonic wave of MSCs in the mouse trunk is neural crest derived (Takashima et al., 2007), it is possible that both the Pparg and RA pathways act via a conserved mechanism to regulate both MSC and neural crest differentiation.

We next investigated whether RA signalling affects other aspects of CNC differentiation at 48 hpf. To ascertain the relative specificity of the RA and DEAB treatments, we looked at differentiation of additional CNC derivatives including iridophores, melanophores, xanthophores, glia, sensory neurons and chondrocytes, as well as muscle (which is mesodermally derived). We found that RA or DEAB treatments commencing after 48 hpf did not have a noticeable effect on these cell types (see Fig. S4 in the supplementary material). In addition, we and others have also found that these cell types are not affected in *nls*^{-/-} fish (Begemann et al., 2001; Kazakova et al., 2006) (data not shown). These data suggest that at this time point, RA signalling acts on CNC to specifically affect the osteoblast and adipocyte cell fate lineages.

Our findings indicate that cephalic adipocytes and osteoblasts share a common precursor cell type (i.e. CNC). However, we did not find evidence that the RA and Pparg pathways mediate the choice between the adipocyte and osteoblast lineages in the same cell (i.e. that there is a bipotent adipo/osteoprogenitor within the CNC population). This is because none of our treatments resulted in the ectopic expression of markers of osteoblast differentiation in place of adipocyte markers, or vice versa. Rather, our data support the model that pre-existing differences in CNC present at 48 hpf cause subpopulations of the CNC to respond differently to Pparg and RA signalling. Nevertheless, our data are only suggestive and resolution of this question will entail single-cell lineage analysis *in vivo*.

Acknowledgements

This work was supported by the Wellcome Trust (072346/Z/03/Z), Cancer Research UK (C11413/A4072), the European Union 'Cells into Organs NoE' and the Medical Research Council (G070091). Deposited in PMC for release after 6 months.

Competing interests statement

The authors declare no competing financial interests.

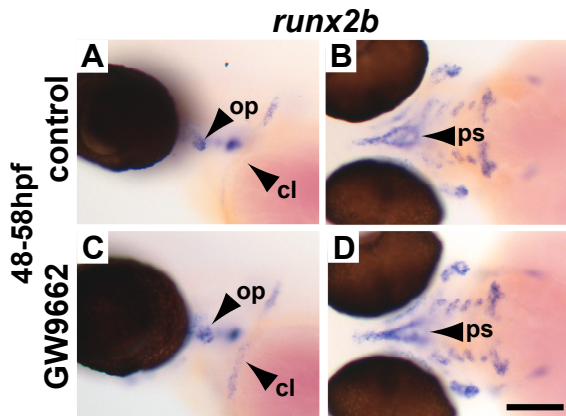
Supplementary material

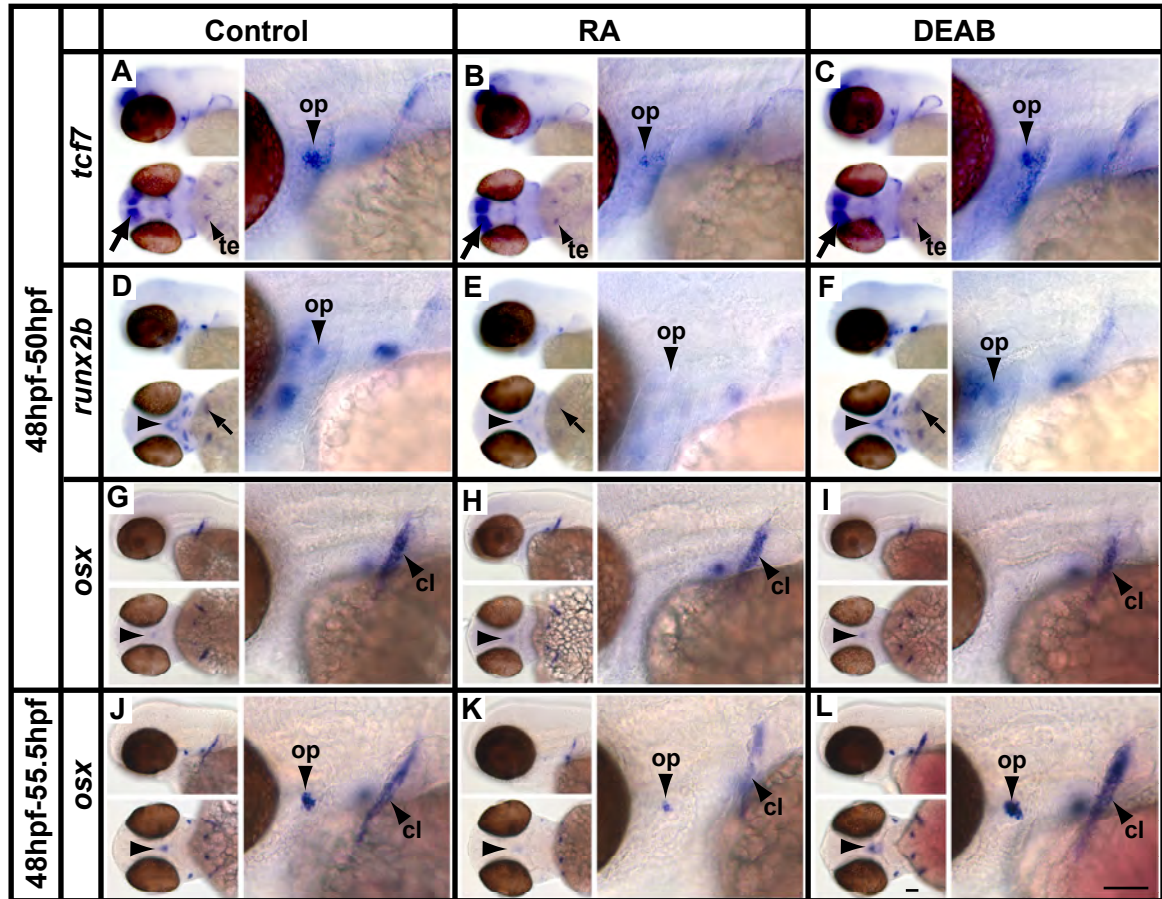
Supplementary material for this article is available at <http://dev.biologists.org/lookup/suppl/doi:10.1242/dev.044164/-/DC1>

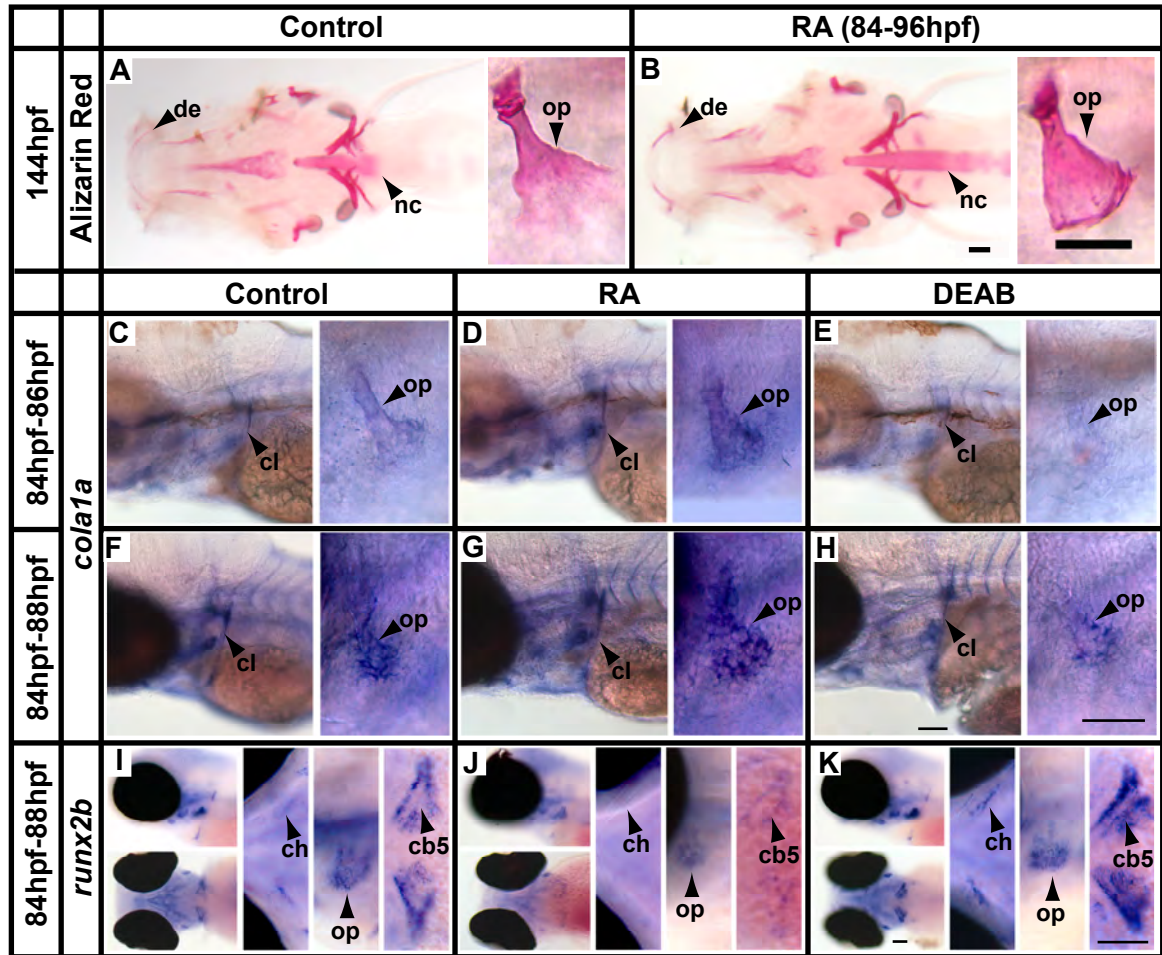
References

- Ahmed, N., Sammons, J., Khokher, M. A. and Hassan, H. T. (2000). Retinoic acid suppresses interleukin 6 production in normal human osteoblasts. *Cytokine* **12**, 289–293.
- Akune, T., Ohba, S., Kamekura, S., Yamaguchi, M., Chung, U. I., Kubota, N., Terauchi, Y., Harada, Y., Azuma, Y., Nakamura, K. et al. (2004). PPARgamma insufficiency enhances osteogenesis through osteoblast formation from bone marrow progenitors. *J. Clin. Invest.* **113**, 846–855.
- Ali, A. A., Weinstein, R. S., Stewart, S. A., Parfitt, A. M., Manolagas, S. C. and Jilka, R. L. (2005). Rosiglitazone causes bone loss in mice by suppressing osteoblast differentiation and bone formation. *Endocrinology* **146**, 1226–1235.
- Allen, S. P., Maden, M. and Price, J. S. (2002). A role for retinoic acid in regulating the regeneration of deer antlers. *Dev. Biol.* **251**, 409–423.
- Begemann, G., Schilling, T. F., Rauch, G. J., Geisler, R. and Ingham, P. W. (2001). The zebrafish neckless mutation reveals a requirement for *raldh2* in mesodermal signals that pattern the hindbrain. *Development* **128**, 3081–3094.
- Begemann, G., Marx, M., Mebus, K., Meyer, A. and Bastmeyer, M. (2004). Beyond the neckless phenotype: influence of reduced retinoic acid signaling on motor neuron development in the zebrafish hindbrain. *Dev. Biol.* **271**, 119–129.
- Benayahu, D., Fried, A., Shamay, A., Cunningham, N., Blumberg, S. and Wientroub, S. (1994). Differential effects of retinoic acid and growth factors on osteoblastic markers and CD10/NEP activity in stromal-derived osteoblasts. *J. Cell. Biochem.* **56**, 62–73.
- Beresford, J. N., Bennett, J. H., Devlin, C., Leboy, P. S. and Owen, M. E. (1992). Evidence for an inverse relationship between the differentiation of adipocytic and osteogenic cells in rat marrow stromal cell cultures. *J. Cell Sci.* **102**, 341–351.
- Bialek, P., Kern, B., Yang, X., Schrock, M., Sosic, D., Hong, N., Wu, H., Yu, K., Ornitz, D. M., Olson, E. N. et al. (2004). A twist code determines the onset of osteoblast differentiation. *Dev. Cell* **6**, 423–435.
- Billon, N., Iannarelli, P., Monteiro, M. C., Glavieux-Pardanaud, C., Richardson, W. D., Kessaris, N., Dani, C. and Dupin, E. (2007). The generation of adipocytes by the neural crest. *Development* **134**, 2283–2292.
- Burkhardt, R., Kettner, G., Bohm, W., Schmidmeier, M., Schlag, R., Frisch, B., Mallmann, B., Eisenmenger, W. and Gilg, T. (1987). Changes in trabecular bone, hematopoiesis and bone marrow vessels in aplastic anemia, primary osteoporosis, and old age: a comparative histomorphometric study. *Bone* **8**, 157–164.
- Carney, T. J., Dutton, K. A., Greenhill, E., Delfino-Machin, M., Dufourcq, P., Blader, P. and Kelsh, R. N. (2006). A direct role for Sox10 in specification of neural crest-derived sensory neurons. *Development* **133**, 4619–4630.
- Choong, P. F., Martin, T. J. and Ng, K. W. (1993). Effects of ascorbic acid, calcitriol, and retinoic acid on the differentiation of preosteoblasts. *J. Orthop. Res.* **11**, 638–647.
- Clement, A., Wiweger, M., von der Hardt, S., Rusch, M. A., Selleck, S. B., Chien, C. B. and Roehl, H. H. (2008). Regulation of zebrafish skeletogenesis by *ext2/dackel* and *papst1/pinscher*. *PLoS Genet.* **4**, e1000136.
- Delfino-Machin, M., Chipperfield, T. R., Rodrigues, F. S. and Kelsh, R. N. (2007). The proliferating field of neural crest stem cells. *Dev. Dyn.* **236**, 3242–3254.
- Dupin, E., Calloni, G., Real, C., Goncalves-Trentin, A. and Le Douarin, N. M. (2007). Neural crest progenitors and stem cells. *C. R. Biol.* **330**, 521–529.
- Fisher, S., Jagadeeswaran, P. and Halpern, M. E. (2003). Radiographic analysis of zebrafish skeletal defects. *Dev. Biol.* **264**, 64–76.
- Flores, M. V., Tsang, V. W., Hu, W., Kalev-Zylinska, M., Postlethwait, J., Crosier, P., Crosier, K. and Fisher, S. (2004). Duplicate zebrafish *runx2* orthologues are expressed in developing skeletal elements. *Gene Expr. Patterns* **4**, 573–581.
- Flynn, E. J., 3rd, Trent, C. M. and Rawls, J. F. (2009). Ontogeny and nutritional control of adipogenesis in zebrafish (*Danio rerio*). *J. Lipid Res.* **50**, 1641–1652.
- Gibert, Y., Gajewski, A., Meyer, A. and Begemann, G. (2006). Induction and pre-patterning of the zebrafish pectoral fin bud requires axial retinoic acid signaling. *Development* **133**, 2649–2659.
- Grey, A. (2008). Skeletal consequences of thiazolidinedione therapy. *Osteoporos. Int.* **19**, 129–137.
- Hong, J. H., Hwang, E. S., McManus, M. T., Amsterdam, A., Tian, Y., Kalmukova, R., Mueller, E., Benjamin, T., Spiegelman, B. M., Sharp, P. A. et al. (2005). TAZ, a transcriptional modulator of mesenchymal stem cell differentiation. *Science* **309**, 1074–1078.
- Kajkenova, O., Lecka-Czernik, B., Gubrij, I., Hauser, S. P., Takahashi, K., Parfitt, A. M., Jilka, R. L., Manolagas, S. C. and Lipschitz, D. A. (1997). Increased adipogenesis and myelopoiesis in the bone marrow of SAMP6, a murine model of defective osteoblastogenesis and low turnover osteopenia. *J. Bone Miner. Res.* **12**, 1772–1779.
- Kanatani, N., Fujita, T., Fukuyama, R., Liu, W., Yoshida, C. A., Moriishi, T., Yamana, K., Miyazaki, T., Toyosawa, S. and Komori, T. (2006). Cbf beta regulates Runx2 function isoform-dependently in postnatal bone development. *Dev. Biol.* **296**, 48–61.
- Kawaguchi, H., Akune, T., Yamaguchi, M., Ohba, S., Ogata, N., Chung, U. I., Kubota, N., Terauchi, Y., Kadowaki, T. and Nakamura, K. (2005). Distinct effects of PPARgamma insufficiency on bone marrow cells, osteoblasts, and osteoclastic cells. *J. Bone Miner. Metab.* **23**, 275–279.
- Kazakova, N., Li, H., Mora, A., Jessen, K. R., Mirsky, R., Richardson, W. D. and Smith, H. K. (2006). A screen for mutations in zebrafish that affect myelin gene expression in Schwann cells and oligodendrocytes. *Dev. Biol.* **297**, 1–13.
- Komori, T., Yagi, H., Nomura, S., Yamaguchi, A., Sasaki, K., Deguchi, K., Shimizu, Y., Bronson, R. T., Gao, Y. H., Inada, M. et al. (1997). Targeted disruption of *Cbfa1* results in a complete lack of bone formation owing to maturational arrest of osteoblasts. *Cell* **89**, 755–764.
- Koo, K. H., Dussault, R., Kaplan, P., Kim, R., Ahn, I. O., Christopher, J., Song, H. R. and Wang, G. J. (1998). Age-related marrow conversion in the proximal metaphysis of the femur: evaluation with T1-weighted MR imaging. *Radiology* **206**, 745–748.

- Lang, M. R., Lapierre, L. A., Frotscher, M., Goldenring, J. R. and Knapik, E. W. (2006). Secretory COPII coat component Sec23a is essential for craniofacial chondrocyte maturation. *Nat. Genet.* **38**, 1198-1203.
- Laue, K., Janicke, M., Plaster, N., Sonntag, C. and Hammerschmidt, M. (2008). Restriction of retinoic acid activity by Cyp26b1 is required for proper timing and patterning of osteogenesis during zebrafish development. *Development* **135**, 3775-3787.
- Le Douarin, N. M., Creuzet, S., Couly, G. and Dupin, E. (2004). Neural crest cell plasticity and its limits. *Development* **131**, 4637-4650.
- Leesnitzer, L. M., Parks, D. J., Bledsoe, R. K., Cobb, J. E., Collins, J. L., Conslor, T. G., Davis, R. G., Hull-Ryde, E. A., Lenhard, J. M., Patel, L. et al. (2002). Functional consequences of cysteine modification in the ligand binding sites of peroxisome proliferator activated receptors by GW9662. *Biochemistry* **41**, 6640-6650.
- Li, N., Felber, K., Elks, P., Croucher, P. and Roehl, H. H. (2009). Tracking gene expression during zebrafish osteoblast differentiation. *Dev. Dyn.* **238**, 459-466.
- Linhart, H. G., Ishimura-Oka, K., DeMayo, F., Kibe, T., Repka, D., Poindexter, B., Bick, R. J. and Darlington, G. J. (2001). C/EBPalpha is required for differentiation of white, but not brown, adipose tissue. *Proc. Natl. Acad. Sci. USA* **98**, 12532-12537.
- Linville, A., Gumusaneli, E., Chandraratna, R. A. and Schilling, T. F. (2004). Independent roles for retinoic acid in segmentation and neuronal differentiation in the zebrafish hindbrain. *Dev. Biol.* **270**, 186-199.
- Liu, R. Z., Saxena, V., Sharma, M. K., Thisse, C., Thisse, B., Denovan-Wright, E. M. and Wright, J. M. (2007). The fabp4 gene of zebrafish (*Danio rerio*)-genomic homology with the mammalian FABP4 and divergence from the zebrafish fabp3 in developmental expression. *FEBS J.* **274**, 1621-1633.
- Manji, S. S., Ng, K. W., Martin, T. J. and Zhou, H. (1998). Transcriptional and posttranscriptional regulation of osteopontin gene expression in preosteoblasts by retinoic acid. *J. Cell. Physiol.* **176**, 1-9.
- Meunier, P., Aaron, J., Edouard, C. and Vignon, G. (1971). Osteoporosis and the replacement of cell populations of the marrow by adipose tissue. A quantitative study of 84 iliac bone biopsies. *Clin. Orthop. Relat. Res.* **80**, 147-154.
- Nakashima, K., Zhou, X., Kunkel, G., Zhang, Z., Deng, J. M., Behringer, R. R. and de Crombrughe, B. (2002). The novel zinc finger-containing transcription factor osterix is required for osteoblast differentiation and bone formation. *Cell* **108**, 17-29.
- Nuttall, M. E. and Gimble, J. M. (2000). Is there a therapeutic opportunity to either prevent or treat osteopenic disorders by inhibiting marrow adipogenesis? *Bone* **27**, 177-184.
- Ohishi, K., Nishikawa, S., Nagata, T., Yamauchi, N., Shinohara, H., Kido, J. and Ishida, H. (1995). Physiological concentrations of retinoic acid suppress the osteoblastic differentiation of fetal rat calvaria cells in vitro. *Eur. J. Endocrinol.* **133**, 335-341.
- Otto, F., Thornell, A. P., Crompton, T., Denzel, A., Gilmour, K. C., Rosewell, I. R., Stamp, G. W., Beddington, R. S., Mundlos, S., Olsen, B. R. et al. (1997). Cbfa1, a candidate gene for cleidocranial dysplasia syndrome, is essential for osteoblast differentiation and bone development. *Cell* **89**, 765-771.
- Phillips, B. W., Vernochet, C. and Dani, C. (2003). Differentiation of embryonic stem cells for pharmacological studies on adipose cells. *Pharmacol. Res.* **47**, 263-268.
- Phinney, D. G. and Prockop, D. J. (2007). Concise review: mesenchymal stem/multipotent stromal cells: the state of transdifferentiation and modes of tissue repair-current views. *Stem Cells* **25**, 2896-2902.
- Rosen, E. D. and MacDougald, O. A. (2006). Adipocyte differentiation from the inside out. *Nat. Rev. Mol. Cell Biol.* **7**, 885-896.
- Schlegel, A. and Stainier, D. Y. (2006). Microsomal triglyceride transfer protein is required for yolk lipid utilization and absorption of dietary lipids in zebrafish larvae. *Biochemistry* **45**, 15179-15187.
- Song, H. M., Nacamuli, R. P., Xia, W., Bari, A. S., Shi, Y. Y., Fang, T. D. and Longaker, M. T. (2005). High-dose retinoic acid modulates rat calvarial osteoblast biology. *J. Cell. Physiol.* **202**, 255-262.
- Song, Y. and Cone, R. D. (2007). Creation of a genetic model of obesity in a teleost. *FASEB J.* **21**, 2042-2049.
- Spoorendonk, K. M., Peterson-Maduro, J., Renn, J., Trowe, T., Kranenborg, S., Winkler, C. and Schulte-Merker, S. (2008). Retinoic acid and Cyp26b1 are critical regulators of osteogenesis in the axial skeleton. *Development* **135**, 3765-3774.
- Takashima, Y., Era, T., Nakao, K., Kondo, S., Kasuga, M., Smith, A. G. and Nishikawa, S. (2007). Neuroepithelial cells supply an initial transient wave of MSC differentiation. *Cell* **129**, 1377-1388.
- Thisse, B., Pflumio, S., Furthauer, M., Loppin, B., Heyer, V., Degraeve, A., Woehl, R., Lux, A., Steffan, T., Charbonnier, X. Q. and Thisse, C. (2001). Expression of the zebrafish genome during embryogenesis. NIH R01 RR15402, ZFIN direct data submission, <http://zfin.org>.
- Thisse, C. and Thisse, B. (2008). High-resolution in situ hybridization to whole-mount zebrafish embryos. *Nat. Protoc.* **3**, 59-69.
- Tontonoz, P., Hu, E. and Spiegelman, B. M. (1994). Stimulation of adipogenesis in fibroblasts by PPAR gamma 2, a lipid-activated transcription factor. *Cell* **79**, 1147-1156.
- Umek, R. M., Friedman, A. D. and McKnight, S. L. (1991). CCAAT-enhancer binding protein: a component of a differentiation switch. *Science* **251**, 288-292.
- van der Meulen, T., Kranenborg, S., Schipper, H., Samallo, J., van Leeuwen, J. L. and Franssen, H. (2005). Identification and characterisation of two runx2 homologues in zebrafish with different expression patterns. *Biochim. Biophys. Acta* **1729**, 105-117.
- Verma, S., Rajaratnam, J. H., Denton, J., Hoyland, J. A. and Byers, R. J. (2002). Adipocytic proportion of bone marrow is inversely related to bone formation in osteoporosis. *J. Clin. Pathol.* **55**, 693-698.
- Weston, A. D., Hoffman, L. M. and Underhill, T. M. (2003). Revisiting the role of retinoid signaling in skeletal development. *Birth Defects Res. C Embryo Today* **69**, 156-173.
- Wipier-Bergeron, N., St-Louis, C. and Lee, J. M. (2007). CCAAT/Enhancer binding protein beta abrogates retinoic acid-induced osteoblast differentiation via repression of Runx2 transcription. *Mol. Endocrinol.* **21**, 2124-2135.
- Yang, D. C., Tsay, H. J., Lin, S. Y., Chiou, S. H., Li, M. J., Chang, T. J. and Hung, S. C. (2008). cAMP/PKA regulates osteogenesis, adipogenesis and ratio of RANKL/OPG mRNA expression in mesenchymal stem cells by suppressing leptin. *PLoS ONE* **3**, e1540.
- Zhao, L. J., Jiang, H., Papisian, C. J., Maulik, D., Drees, B., Hamilton, J. and Deng, H. W. (2008). Correlation of obesity and osteoporosis: effect of fat mass on the determination of osteoporosis. *J. Bone Miner. Res.* **23**, 17-29.







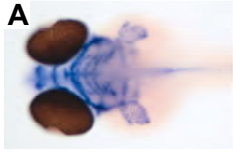

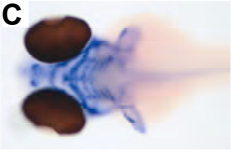
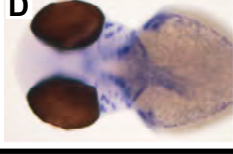

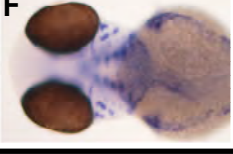






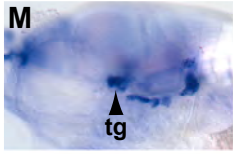
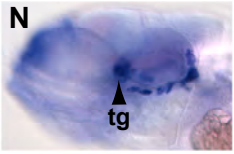
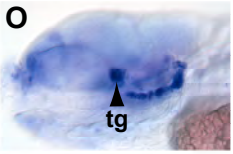



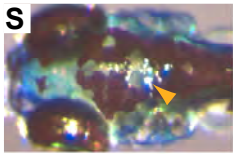
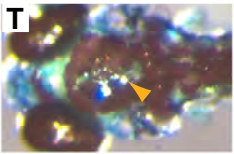
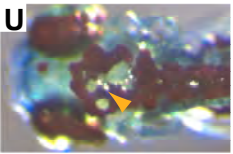
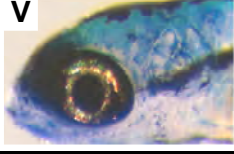
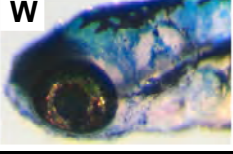
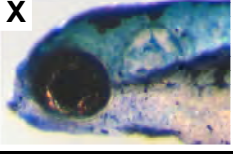
	DMSO	RA	DEAB
<i>sox9a</i> 60hpf	48-60hpf A 	48-60hpf B 	48-60hpf C 
	<i>myod</i> 60hpf D 	E 	F 
Alcian Blue 120hpf	48-120hpf G 	48-60hpf H 	48-120hpf I 
	<i>anti-sarcomere</i> 96hpf J 	K 	L 
<i>mbp</i> 100hpf	48-100hpf M  tg	48-54hpf N  tg	48-100hpf O  tg
	P  tg	Q  tg	R  tg
live larvae 124hpf	48-124hpf S  ▲	48-54hpf T  ▲	48-124hpf U  ▲
	V 	W 	X 

Table S1. Alizarin Red after GW9662 treatment

	Control (<i>n</i> =15)	GW9662 (<i>n</i> =15)
Ceratohyal	0	4
Hyomandibular	0	8
Maxilla and dentary	0	7

GW9662 at 5 μ M 48-120 hpf.

Table S2. Alizarin Red after RA pulse treatment

	Control (n=20)	48-54 hpf (n=20)
Branchiostegal ray	20	20
Opercle	20	20
Cleithrum	20	20
Entopterygoid	18	3
Hyomandibular	17	18
Ceratohyal	19	18
Maxilla and dentary	20	1

RA 0.5 μ M pulse 48-54 hpf (fix at 144 hpf).

Table S3. Alizarin Red after DEAB pulse treatment

	Control (<i>n</i> =14)	48-54 hpf (<i>n</i> =15)	48-60 hpf (<i>n</i> =15)	48-72 hpf (<i>n</i> =10)
Branchiostegal ray	14	15	15	10
Opercle	14	15	15	10
Cleithrum	14	15	15	10
Entopterygoid	5	11	12	5
Hyomandibular	2	9	11	5
Ceratohyal	0	6	11	3
Maxilla and dentary	0	10	12	7

DEAB 10 μ M pulse (fix at 120 hpf).